Geomechanics and Engineering, *Vol. 10, No. 1 (2016) 59-76*
DOI: http://dx.doi.org/10.12989/gae.2016.10.1.059

Limit analysis of 3D rock slope stability with non-linear failure criterion

Yufeng Gao [1], Di Wu [1], Fei Zhang [*1], G.H. Lei [1], Hongyu Qin [2] and Yue Qiu [1]

[1] *Key Laboratory of Ministry of Education for Geomechanics and Embankment Engineering, Hohai University, Nanjing, 210098, China*
[2] *School of Computer Science, Engineering and Mathematics, Flinders University, Adelaide, SA 5001, Australia*

(*Received August 12, 2014, Revised July 26, 2015, Accepted November 15, 2015*)

Abstract. The non-linear Hoek–Brown failure criterion has been widely accepted and applied to evaluate the stability of rock slopes under plane-strain conditions. This paper presents a kinematic approach of limit analysis to assessing the static and seismic stability of three-dimensional (3D) rock slopes using the generalized Hoek–Brown failure criterion. A tangential technique is employed to obtain the equivalent Mohr–Coulomb strength parameters of rock material from the generalized Hoek–Brown criterion. The least upper bounds to the stability number are obtained in an optimization procedure and presented in the form of graphs and tables for a wide range of parameters. The calculated results demonstrate the influences of 3D geometrical constraint, non-linear strength parameters and seismic acceleration on the stability number and equivalent strength parameters. The presented upper-bound solutions can be used for preliminary assessment on the 3D rock slope stability in design and assessing other solutions from the developing methods in the stability analysis of 3D rock slopes.

Keywords: limit analysis; rock slope; three-dimensional; stability; failure criterion

1. Introduction

Analysis of rock slope stability remains an active and important area of study for geotechnical and mining engineers. In the traditional approaches to assessing the safety of rock slopes (e.g., the limit equilibrium method and the limit analysis method), the linear Mohr–Coulomb (MC) failure criterion has been used to estimate the strength of rock masses. However, a large number of experiments have demonstrated that the strength envelope of rock masses is non-linear. Various non-linear failure criteria for rocks have been presented, such as Hobbs (1966), Hoek and Brown (1980), Yudhbir *et al*. (1983) and Sheorey *et al*. (1989). Among these non-linear criteria, the Hoek–Brown (HB) failure criterion is widely accepted and utilized to solve a large number of rock engineering problems, such as underground excavation (e.g., Carranza-Torres and Fairhurst 1999, Sharan 2003, Fraldi and Guarracino 2009, Yang and Qin 2014) and slope stability (e.g., Collins *et al*. 1988, Dawson *et al*. 2000, Yang *et al*. 2004, Li *et al*. 2008, Saada *et al*. 2012).

Many attempts have been made to apply the non-linear HB failure criterion into the stability analysis of rock slopes. Hoek *et al*. (2002) presented the equivalent MC strength parameters using

*Corresponding author, Ph.D., E-mail: geofeizhang@gmail.com

http://www.techno-press.org/?journal=gae&subpage=5 ISSN: 2005-307X (Print), 2092-6219 (Online)

simply linearly fitting the HB strength envelope. Such an approach was incorporated into the conventional limit equilibrium method by Li *et al*. (2008) and Lin *et al*. (2014). Carranza-Torres (2004) and Shen *et al*. (2013) also combined the limit equilibrium method with a generic form of the HB criterion to analyze the rock slope stability. Based on the limit analysis method, Collins *et al*. (1988), Yang *et al*. (2004) and Saada *et al*. (2012) applied the HB criterion into the upper-bound analysis of rock slope stability. In addition, the HB failure criterion has also been utilized into other numerical methods such as the finite-element limit analysis method (Li *et al*. 2008, 2009), the finite element method (Hammah *et al*. 2004, Fu and Liao 2010, Chakraborti *et al*. 2012, Shen and Karakus 2013) and the finite difference method (Dawson *et al*. 2000). Nevertheless, most of these studies are limited to the two-dimensional (2D) rock slopes and the 2D solutions will underestimate the stability of a 3D rock slope. Based on the HB criterion, Shen and Karakus (2013) proposed a 3D numerical method for the stability analysis of 3D rock slopes. Their study investigated the effects of the convergence criterion and boundary conditions on the 3D slope modeling, but little attention was paid to the 3D geometrical effect and the nonlinearity of rock masses. Therefore, it is significantly necessary to perform 3D slope stability analysis using the non-linear HB failure criterion to demonstrate the influences of 3D geometrical constraint and non-linear strength parameters on the stability of actual rock slopes.

In the strict framework of upper-bound limit analysis, Michalowski and Drescher (2009) have recently presented a 3D rotational failure mechanism for a slope in frictional/cohesive soils satisfying MC failure criterion. The method has been used to investigate the 3D effect on the stability of earth slopes subjected to excavations (Michalowski and Drescher 2009) and seismic excitations (Michalowski and Martel 2011). In this paper, the tangential technique, that has been found effective in the limit analysis of 2D rock slope stability (Collins *et al*. 1988, Yang *et al*. 2004), is adopted to obtain the equivalent MC strength parameters. And then the kinematic approach of limit analysis proposed by Michalowski and Drescher (2009) is used to estimate the stability of 3D slopes in rock masses obeying the generalized HB failure criterion.

2. Limit analysis of 3D rock slope stability

2.1 The generalized Hoek–Brown failure criterion

Hoek and Brown (1980) earlier proposed a non-linear failure criterion for estimating the strength of intact rock or heavily jointed rock masses, and then Hoek (1983) and Hoek *et al*. (1992, 2002) further developed and improved the criterion. The latest version is the generalized HB failure criterion given by Hoek *et al*. (2002), as follows

$$\sigma_1' = \sigma_3' + \sigma_{ci}\left(m_b\frac{\sigma_3'}{\sigma_{ci}} + s\right)^{\alpha} \tag{1}$$

where σ_1' and σ_3' are the major and minor effective principal stresses at failure, respectively; and σ_{ci} is the intact uniaxial compressive strength. The strength parameters m_b, s and α are defined as

$$m_b = m_i\exp\left(\frac{GSI-100}{28-14D}\right) \tag{2}$$

$$s = \exp\left(\frac{GSI - 100}{9 - 3D}\right) \tag{3}$$

$$\alpha = \frac{1}{2} + \frac{1}{6}\left(e^{-GSI/15} - e^{-20/3}\right) \tag{4}$$

where *GSI* is the geological strength index ranging from 10 for extremely poor rock masses to 100 for intact rock. *D* is a disturbance factor varying from 0 for undisturbed in situ rock masses to 1 for very disturbed rock masses. In this study, the disturbance factor $D = 0$ is adopted here. m_i is the material constant. If there are no available test data, Hoek (2007) presented the approximate values of m_i for five rock types:

(a) $m_i = 7$ for carbonate rocks with well-developed crystal cleavage (dolomite, limestone and marble)
(b) $m_i = 10$ for lithified argillaceous rocks (mudstone, shale and slate(normal to cleavage))
(c) $m_i = 15$ for arenaceous rocks with strong crystals and poorly-developed crystal cleavage (sandstone and quartzite)
(d) $m_i = 17$ for fine grained polyminerallic igneous crystalline rocks (andesite, dolerite, diabase and rhyolite)
(e) $m_i = 25$ for coarse grained polyminerallic igneous and metamorphic rocks (amphibolite, gabbro, gneiss, granite, norite and qranodiorite).

For more details of the description of the generalized HB failure criterion, see the source reference (Hoek *et al*. 2002).

2.2 The tangential technique

Based on the kinematic approach of limit analysis, Collins *et al*. (1988) and Yang *et al*. (2004) adopted the tangential technique to derive the upper-bound solutions for the stability of 2D slopes in rock masses obeying the non-linear HB failure criterion. The tangential equation of the generalized HB failure envelope at the tangency point *P*, shown in Fig. 1, can be expressed as

$$\tau = c_t + \sigma_n \tan\phi_t \tag{5}$$

where τ and σ_n are the shear and normal components of the stress vector, respectively; ϕ_t is the equivalent friction angle; and c_t is the equivalent cohesion. As Yang *et al*. (2004) presented, the equivalent cohesion c_t can be expressed as

$$\begin{aligned}\frac{c_t}{\sigma_{ci}} = {} & \frac{\cos\phi_t}{2}\left[\frac{m_b\alpha\left(1-\sin\phi_t\right)}{2\sin\phi_t}\right]^{\left(\frac{\alpha}{1-\alpha}\right)} \\ & -\frac{\tan\phi_t}{m_b}\left(1+\frac{\sin\phi_t}{\alpha}\right)\left[\frac{m_b\alpha\left(1-\sin\phi_t\right)}{2\sin\phi_t}\right]^{\left(\frac{1}{1-\alpha}\right)} + \frac{s}{m_b}\tan\phi_t\end{aligned} \tag{6}$$

It can be seen that the expression of c_t is a function of ϕ_t. The equivalent friction angle ϕ_t is regarded as one of the variables determining the shape of the failure mechanism and the location of tangency line to the HB criterion. The value of ϕ_t can be obtained in the search for the least upper bound to the stability number for slopes.

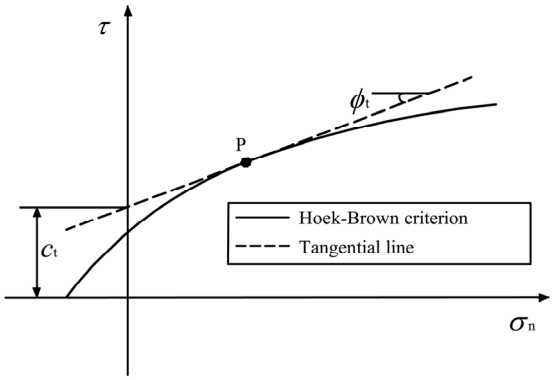

Fig. 1 The tangential line based on the HB failure criterion

2.3 Kinematic approach with 3D rotational failure mechanism

According to the theorem of limit analysis, Michalowski and Drescher (2009) proposed a 3D admissible rotational failure mechanism for slopes in frictional/cohesive soils obeying MC failure criterion. The rotational mechanism is limited to slopes in homogeneous and isotropic materials. The generalized HB failure criterion is developed to estimate the strength of homogeneous and isotropic rock material. Therefore, the mechanism can be appropriately used to analyze the stability of 3D slopes in intact rock or heavily jointed rock masses with the generalized HB criterion.

The 3D rotational failure mechanism presented by Michalowski and Drescher (2009) is

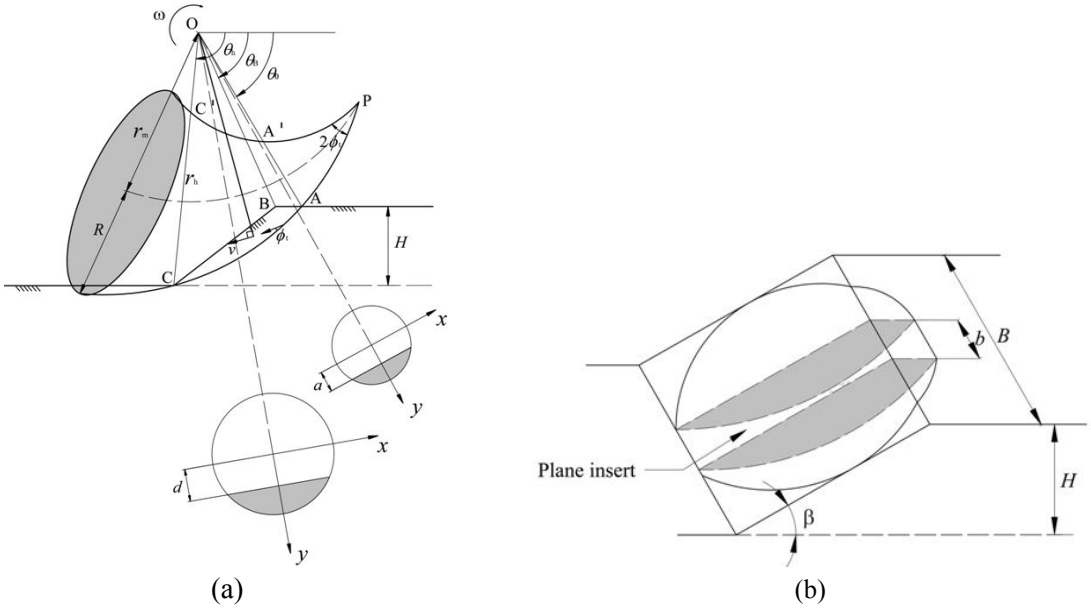

Fig. 2 3D rotational failure mechanism: (a) a 'horn-shape' surface; (b) failure surface with limited width B (adopted from Michalowski and Drescher (2009))

illustrated in Fig. 2(a) as a 'horn-shape' surface. Fig. 2(b) shows the mechanism for the slope with finite width B modified by adding a plane insert of width b, to allow the transition to the 2D log-spiral failure mechanism as b approaches infinity. Details of the construction of the 3D admissible rotational failure mechanism can be found in the source reference.

Based on the 3D failure mechanism, the upper bound to the stability number $N = \gamma H/\sigma_{ci}$ (γ is the unit weight of rock masses; H is the slope height) can be determined by equating the rate of work W_γ done by rock masses weight to the rate of internal energy dissipation W_d. It should be noted that the stability number $\gamma H/\sigma_{ci}$ is defined as a dimensionless critical height, when the value of safety factor is equal to 1.0. To account for the effect of horizontal seismic forces on slope stability, an additional rate of work W_s done by the pseudo-static seismic loading $k_h\gamma$ (k_h is the horizontal seismic acceleration coefficient) is counted into the energy balance equation. In general, the balance equation is given as follows

$$W_\gamma^{\text{curve}} + W_\gamma^{\text{plane}} + W_s^{\text{curve}} + W_s^{\text{plane}} = W_d^{\text{curve}} + W_d^{\text{plane}} \tag{7}$$

where the superscript 'curve' denotes the work rates for a section of the curvilinear cone at the two ends of the mechanism and the superscript 'plane' relates to the plane insert in the center of the mechanism. The expressions of W_γ^{plane}, W_s^{plane} and W_d^{plane} for the plane insert can be found in the references (e.g., Chen and Liu 1990, Michalowski and You 2000). The expressions of W_γ^{curve}, W_s^{curve} and W_d^{curve} for the two ends can be derived from Michalowski and Drescher (2009) and Michalowski and Martel (2011), as

$$\begin{aligned} W_\gamma^{\text{curve}} = 2\omega\gamma \Bigg[& \int_{\theta_0}^{\theta_B} \int_0^{\sqrt{R^2-a^2}} \int_a^{\sqrt{R^2-x^2}} \left(r_m + y\right)^2 \cos\theta \,\mathrm{d}y\mathrm{d}x\mathrm{d}\theta \\ & + \int_{\theta_B}^{\theta_h} \int_0^{\sqrt{R^2-d^2}} \int_d^{\sqrt{R^2-x^2}} \left(r_m + y\right)^2 \cos\theta \,\mathrm{d}y\mathrm{d}x\mathrm{d}\theta \Bigg] \end{aligned} \tag{8}$$

$$\begin{aligned} W_s^{\text{curve}} = 2\omega k_h\gamma \Bigg[& \int_{\theta_0}^{\theta_B} \int_0^{\sqrt{R^2-a^2}} \int_a^{\sqrt{R^2-x^2}} \left(r_m + y\right)^2 \sin\theta \,\mathrm{d}y\mathrm{d}x\mathrm{d}\theta \\ & + \int_{\theta_B}^{\theta_h} \int_0^{\sqrt{R^2-d^2}} \int_d^{\sqrt{R^2-x^2}} \left(r_m + y\right)^2 \sin\theta \,\mathrm{d}y\mathrm{d}x\mathrm{d}\theta \Bigg] \end{aligned} \tag{9}$$

$$\begin{aligned} W_d^{\text{curve}} = \frac{2c_t\omega r_0^2}{\tan\phi_t} \Bigg[& \left(-\sin^2\theta_0 \int_{\theta_0}^{\theta_B} \frac{\cos\theta}{\sin^3\theta} \sqrt{R^2 - a^2}\,\mathrm{d}\theta \right) \\ & + \left(-\sin^2\left(\beta + \theta_h\right) e^{2(\theta_h - \theta_0)\tan\phi_t} \int_{\theta_B}^{\theta_h} \frac{\cos\left(\theta + \beta\right)}{\sin^3\left(\theta + \beta\right)} \sqrt{R^2 - d^2}\,\mathrm{d}\theta \right) \Bigg] \end{aligned} \tag{10}$$

Similar symbols were used by Michalowski and Drescher (2009). For details of the procedure and notation, see the reference of Michalowski and Drescher (2009). It should be noted that c_t is a function of ϕ_t determined by Eq. (6).

According to the balance Eq. (7), the least upper bound to the stability number $\gamma H/\sigma_{ci}$ can be obtained from an optimization procedure of Chen (1992). The optimization procedure uses random

search to find the global minimum value based on a computer program. In the search for the minimum value of $\gamma H/\sigma_{ci}$, four independent geometrical variables angles θ_0, θ_h, ratio r_0'/r_0, relative width of the plane insert b/H, and one additional variable ϕ_t are included in the optimization procedure.

3. Results and discussions

3.1 The stability number

Figs. 3-6 show the critical values of $\gamma H/\sigma_{ci}$ for rock slopes with various ratios of B/H (1, 2, 3, 5) and a range of the parameter GSI (10, 50, 100) under both static ($k_h = 0$) and pseudo-static seismic loading conditions. The charts are presented as a function of the parameter m_i. The lowest curves marked by '2D' in each chart represent the stability number for the 2D log-spiral mechanism of Chen (1975). As expected, the stability number $\gamma H/\sigma_{ci}$ increases with increasing GSI, and it reduces with increasing ratio of B/H, slope angle β and seismic acceleration coefficient k_h. The

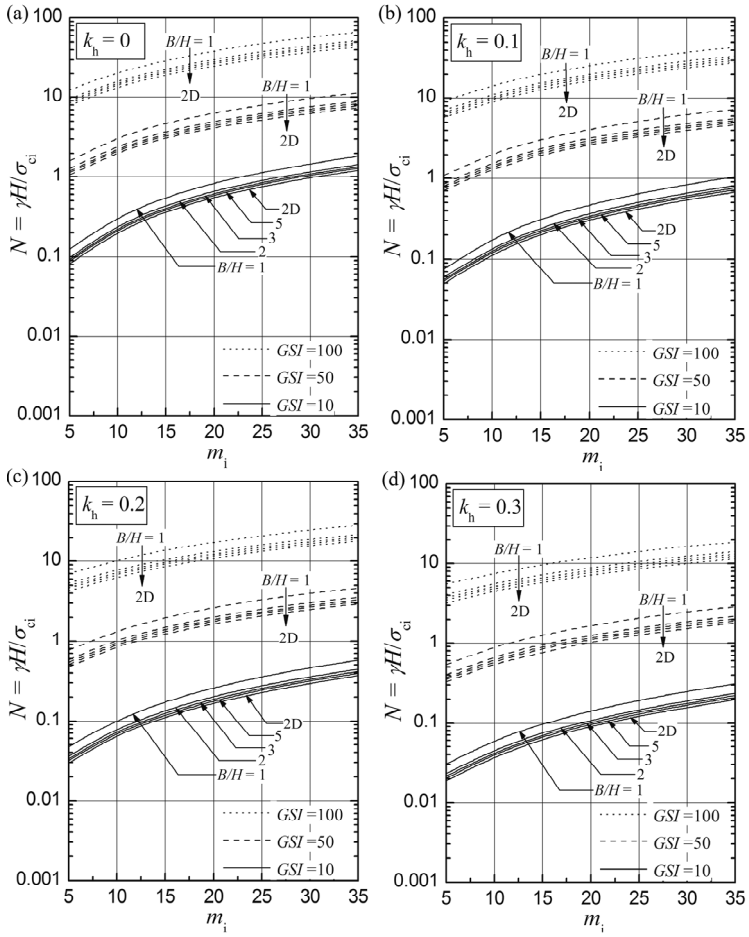

Fig. 3 The critical values of $\gamma H/\sigma_{ci}$ for rock slopes ($\beta = 45°$) with various ratios of B/H

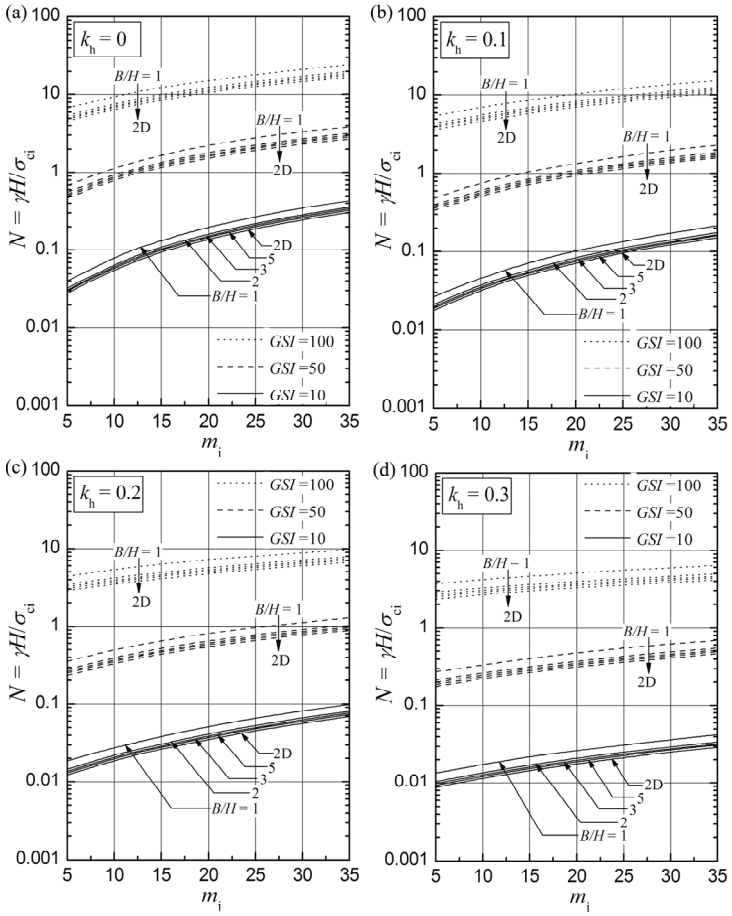

Fig. 4 The critical values of $\gamma H/\sigma_{ci}$ for rock slopes ($\beta = 60°$) with various ratios of B/H

stability number obviously increases as m_i increases in most cases, except for steep slopes, as shown in Figs. 5 and 6. For steep slopes ($\beta = 75°$) subjected to strong seismic loadings, the stability number decreases very slightly with increasing m_i, as shown in Fig. 5(d). This is in good agreement with the 2D results presented by Li *et al*. (2009). However, for vertical slopes under seismic loadings, a significant decrease in the stability number can be found in Figs. 6(b)-(d). Selecting a vertical slope with given values ($GSI = 100$, $B/H = 3$ and $k_h = 0.3$) as an example, the HB failure criteria and tangency points for variable m_i are presented in Fig. 7. When the normal stress is smaller than a certain value, the rock masses with a larger m_i can provide less shear strength. For steep slopes, the slope slip surfaces are rather shallow, and their normal stresses along the slip surface are relatively smaller. Therefore, as m_i increases, the stability number for steep slopes decreases because of less shear strength provided.

The difference in stability numbers between the 2D and 3D analysis is shown in Table 1 for rock slopes ($\beta = 60°$) with four kinds of rock masses. It can be seen that the difference decreases with increasing ratio of B/H, but increases with increasing k_h. Typically, once the constraint on the width of the slope reaches $B/H = 10.0$, the difference is less than 5%. The plane-strain analysis is

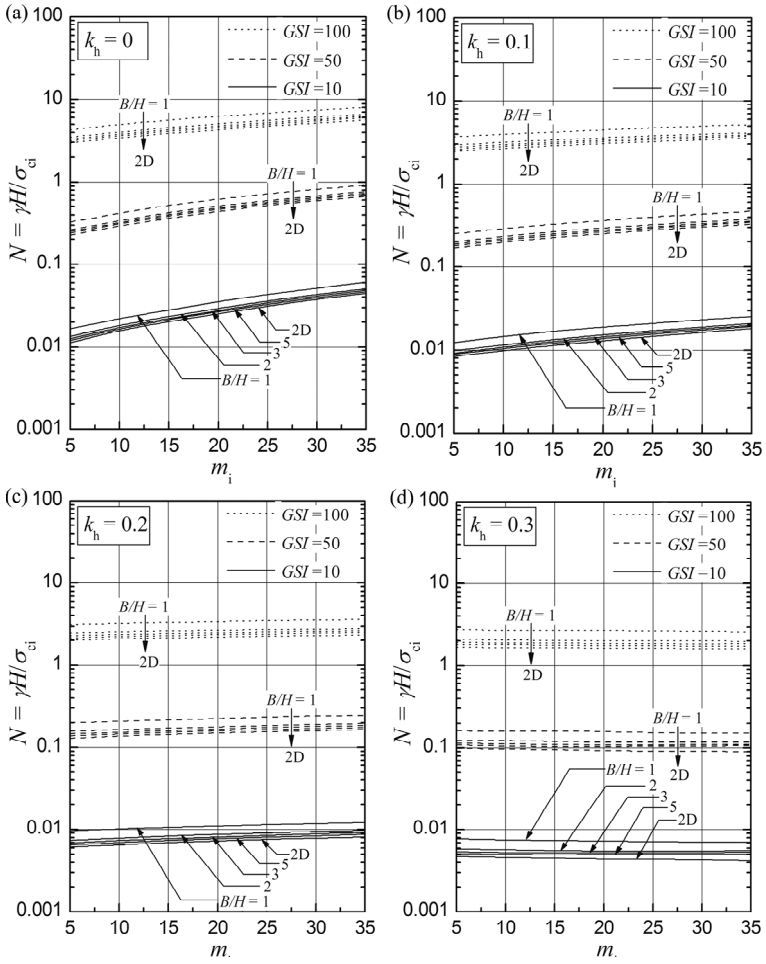

Fig. 5 The critical values of $\gamma H/\sigma_{ci}$ for rock slopes ($\beta = 75°$) with various ratios of B/H

Table 1 The difference in stability numbers between the 2D and 3D analysis ($\beta = 60°$)

k_h	GSI	m_i	B/H				
			1.0	2.0	3.0	5.0	10.0
0	10	10	41.38%	15.52%	8.62%	5.17%	1.72%
	10	35	41.17%	16.07%	10.20%	5.64%	2.71%
	100	10	45.07%	17.62%	11.02%	6.16%	2.96%
	100	35	43.10%	16.85%	10.40%	5.90%	2.82%
0.3	10	10	51.52%	19.48%	11.69%	6.49%	3.20%
	10	35	46.90%	18.28%	11.72%	7.59%	4.14%
	100	10	57.94%	21.86%	13.33%	7.49%	3.36%
	100	35	51.90%	19.25%	11.75%	6.58%	3.18%

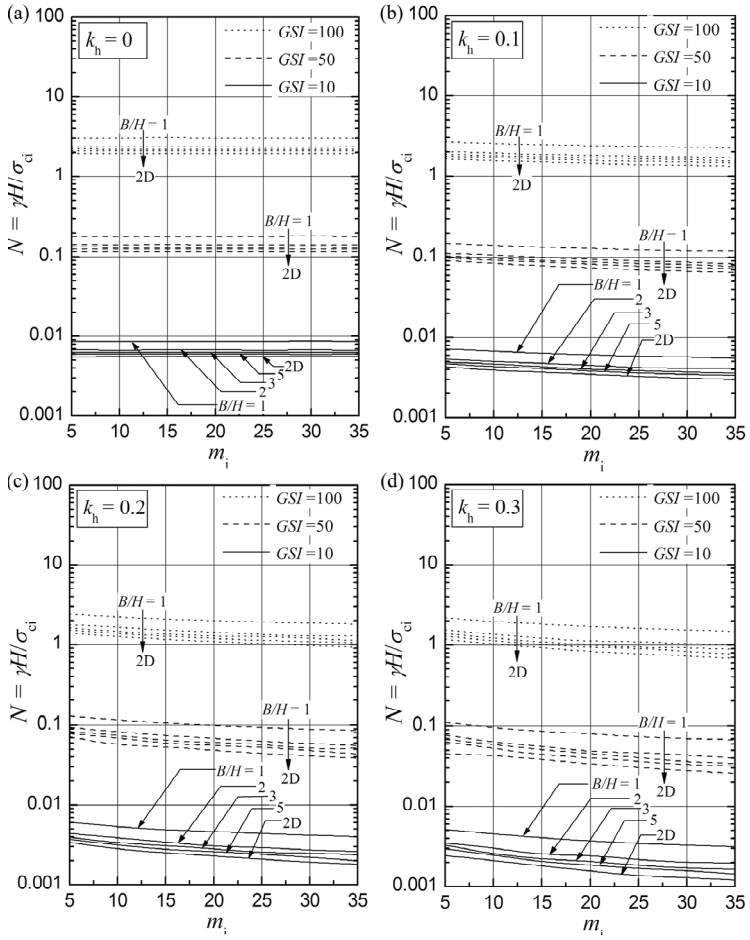

Fig. 6 The critical values of $\gamma H/\sigma_{ci}$ for rock slopes ($\beta = 90°$) with various ratios of B/H

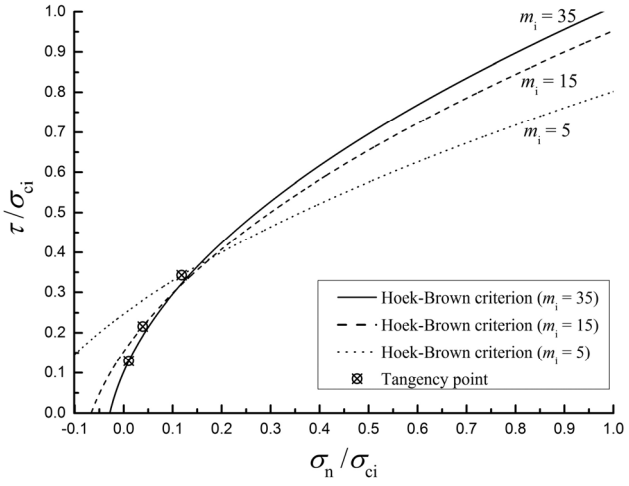

Fig. 7 Hoek-Brown failure criteria for variable m_i

Table 2 The values of the stability number for rock slopes with $m_i = 7$

β	GSI	B/H						
		1.0	1.5	2.0	3.0	5.0	10.0	2D
45°	10	0.196	0.166	0.154	0.144	0.137	0.133	0.129
	20	0.517	0.438	0.408	0.381	0.362	0.350	0.338
	50	2.242	1.897	1.764	1.645	1.565	1.511	1.463
	80	7.072	5.984	5.566	5.187	4.931	4.760	4.605
	90	10.449	8.837	8.205	7.656	7.279	7.025	6.794
	100	15.567	13.174	12.223	11.407	10.841	10.461	10.116
60°	10	0.055	0.048	0.045	0.042	0.041	0.040	0.039
	20	0.166	0.144	0.135	0.128	0.123	0.119	0.116
	50	0.870	0.754	0.709	0.669	0.641	0.622	0.605
	80	3.182	2.764	2.581	2.434	2.330	2.260	2.195
	90	4.966	4.292	4.024	3.792	3.628	3.517	3.416
	100	7.833	6.774	6.342	5.970	5.710	5.534	5.371
75°	10	0.019	0.016	0.015	0.014	0.014	0.013	0.013
	20	0.055	0.048	0.045	0.043	0.041	0.040	0.039
	50	0.363	0.315	0.296	0.280	0.268	0.260	0.253
	80	1.658	1.434	1.344	1.266	1.214	1.174	1.140
	90	2.759	2.403	2.237	2.100	2.009	1.946	1.888
	100	4.626	3.994	3.754	3.504	3.346	3.241	3.143
90°	10	0.009	0.007	0.007	0.006	0.006	0.006	0.006
	20	0.024	0.020	0.019	0.017	0.017	0.016	0.015
	50	0.181	0.153	0.141	0.132	0.126	0.121	0.116
	80	0.989	0.834	0.773	0.722	0.683	0.661	0.636
	90	1.735	1.461	1.350	1.267	1.193	1.151	1.109
	100	3.015	2.545	2.357	2.194	2.083	2.003	1.932

Table 3 The values of the stability number for rock slopes with $m_i = 10$

β	GSI	B/H						
		1.0	1.5	2.0	3.0	5.0	10.0	2D
45°	10	0.319	0.270	0.251	0.235	0.224	0.216	0.209
	20	0.783	0.663	0.617	0.576	0.548	0.530	0.513
	50	3.180	2.695	2.499	2.336	2.222	2.146	2.076
	80	9.721	8.226	7.651	7.133	6.785	6.551	6.338
	90	14.170	11.982	11.121	10.414	9.875	9.533	9.223
	100	20.753	17.572	16.297	15.219	14.467	13.965	13.509

Table 3 Continued

β	*GSI*	*B*/*H*						
		1.0	1.5	2.0	3.0	5.0	10.0	2D
60°	10	0.082	0.071	0.067	0.063	0.061	0.059	0.058
	20	0.239	0.208	0.195	0.185	0.177	0.172	0.168
	50	1.167	1.013	0.952	0.899	0.863	0.838	0.815
	80	4.007	3.470	3.280	3.074	2.945	2.858	2.778
	90	6.131	5.295	4.970	4.686	4.489	4.354	4.231
	100	9.451	8.172	7.663	7.233	6.916	6.708	6.515
75°	10	0.022	0.019	0.018	0.017	0.016	0.016	0.016
	20	0.067	0.058	0.055	0.052	0.050	0.048	0.047
	50	0.420	0.365	0.344	0.325	0.312	0.303	0.295
	80	1.838	1.598	1.493	1.409	1.352	1.311	1.273
	90	3.020	2.611	2.452	2.313	2.213	2.145	2.084
	100	5.034	4.322	4.043	3.812	3.646	3.533	3.430
90°	10	0.009	0.007	0.007	0.006	0.006	0.006	0.006
	20	0.024	0.020	0.019	0.017	0.017	0.016	0.015
	50	0.181	0.154	0.142	0.132	0.125	0.121	0.117
	80	0.988	0.833	0.774	0.719	0.683	0.660	0.636
	90	1.726	1.454	1.357	1.279	1.195	1.150	1.109
	100	3.008	2.538	2.353	2.193	2.078	2.007	1.933

appropriate for 3D slopes with large constraint on the width ($B/H \geq 10.0$). However, the difference between 2D and 3D solutions can exceed 40% when the slope is constrained to a narrow width of $B/H = 1.0$. In this situation, using the 2D solutions will largely underestimate the stability of a 3D rock slope.

Tables 2-6 present the stability numbers for 3D slopes with five types of rock masses (m_i =7, 10, 15, 17, 25) in a range of values of *GSI*, β and *B*/*H*. These tables are presented for preliminary assessment on the stability of a 3D rock slope in design or excavation.

Table 4 The values of the stability number for rock slopes with $m_i = 15$

β	*GSI*	*B*/*H*						
		1.0	1.5	2.0	3.0	5.0	10.0	2D
45°	10	0.560	0.475	0.442	0.413	0.394	0.381	0.369
	20	1.263	1.075	0.994	0.930	0.886	0.855	0.828
	50	4.776	4.042	3.759	3.507	3.337	3.223	3.119
	80	14.252	12.064	11.214	10.465	9.955	9.613	9.301
	90	20.544	17.387	16.158	15.078	14.342	13.849	13.401
	100	29.767	25.166	23.358	21.839	20.749	20.036	19.386

Table 4 The values of the stability number for rock slopes with $m_i = 15$

β	GSI	B/H						
		1.0	1.5	2.0	3.0	5.0	10.0	2D
60°	10	0.136	0.119	0.112	0.106	0.102	0.099	0.096
	20	0.378	0.325	0.306	0.290	0.278	0.270	0.263
	50	1.686	1.468	1.378	1.302	1.249	1.213	1.180
	80	5.457	4.726	4.440	4.194	4.021	3.903	3.795
	90	8.165	7.045	6.619	6.250	5.987	5.812	5.650
	100	12.255	10.611	9.961	9.403	9.006	8.741	8.495
75°	10	0.028	0.025	0.023	0.022	0.021	0.021	0.020
	20	0.087	0.076	0.072	0.068	0.065	0.064	0.062
	50	0.516	0.451	0.424	0.402	0.386	0.376	0.366
	80	2.129	1.849	1.737	1.642	1.576	1.530	1.488
	90	3.441	2.983	2.810	2.647	2.540	2.463	2.395
	100	5.620	4.886	4.556	4.300	4.119	3.997	3.884
90°	10	0.009	0.007	0.007	0.006	0.006	0.006	0.006
	20	0.024	0.020	0.019	0.017	0.017	0.016	0.015
	50	0.180	0.152	0.143	0.131	0.125	0.121	0.117
	80	0.996	0.835	0.775	0.718	0.682	0.660	0.636
	90	1.728	1.452	1.351	1.260	1.197	1.148	1.109
	100	3.037	2.530	2.348	2.199	2.076	2.002	1.934

Table 5 The values of the stability number for rock slopes with $m_i = 17$

β	GSI	B/H						
		1.0	1.5	2.0	3.0	5.0	10.0	2D
45°	10	0.667	0.566	0.526	0.495	0.469	0.454	0.439
	20	1.465	1.242	1.154	1.078	1.027	0.992	0.960
	50	5.419	4.593	4.260	3.981	3.787	3.658	3.540
	80	16.085	13.615	12.642	11.841	11.239	10.853	10.499
	90	23.140	19.588	18.194	16.990	16.175	15.600	15.097
	100	33.396	28.262	26.277	24.513	23.320	22.512	21.780
60°	10	0.161	0.140	0.132	0.125	0.120	0.117	0.114
	20	0.431	0.375	0.353	0.335	0.321	0.312	0.304
	50	1.899	1.651	1.551	1.467	1.410	1.367	1.330
	80	6.046	5.245	4.927	4.654	4.465	4.334	4.215
	90	8.959	7.770	7.295	6.891	6.607	6.412	6.235
	100	13.475	11.617	10.909	10.300	9.868	9.578	9.310

Table 5 Continued

β	*GSI*	*B*/*H*						
		1.0	1.5	2.0	3.0	5.0	10.0	2D
75°	10	0.031	0.027	0.026	0.024	0.024	0.023	0.022
	20	0.095	0.083	0.079	0.075	0.072	0.070	0.068
	50	0.556	0.487	0.457	0.433	0.416	0.405	0.395
	80	2.253	1.958	1.852	1.734	1.664	1.617	1.573
	90	3.608	3.133	2.953	2.779	2.667	2.589	2.518
	100	5.843	5.064	4.761	4.490	4.305	4.178	4.061
90°	10	0.009	0.007	0.007	0.006	0.006	0.006	0.006
	20	0.024	0.020	0.019	0.017	0.017	0.016	0.015
	50	0.181	0.152	0.141	0.133	0.125	0.120	0.117
	80	0.989	0.842	0.770	0.718	0.685	0.659	0.636
	90	1.731	1.448	1.346	1.257	1.194	1.150	1.110
	100	3.050	2.535	2.342	2.188	2.086	2.006	1.934

Table 6 The values of the stability number for rock slopes with $m_i = 25$

β	*GSI*	*B*/*H*						
		1.0	1.5	2.0	3.0	5.0	10.0	2D
45°	10	1.148	0.974	0.905	0.847	0.807	0.780	0.756
	20	2.316	1.962	1.823	1.705	1.623	1.568	1.518
	50	8.018	6.787	6.312	5.891	5.605	5.412	5.238
	80	23.504	19.876	18.463	17.307	16.398	15.839	15.326
	90	33.633	28.486	26.458	24.700	23.492	22.675	21.942
	100	48.262	40.827	37.907	35.420	33.688	32.527	31.478
60°	10	0.271	0.237	0.223	0.211	0.203	0.197	0.192
	20	0.675	0.591	0.553	0.524	0.503	0.489	0.475
	50	2.767	2.409	2.269	2.138	2.052	1.993	1.939
	80	8.489	7.375	6.933	6.549	6.291	6.104	5.934
	90	12.387	10.755	10.101	9.555	9.153	8.888	8.645
	100	18.195	15.787	14.822	14.005	13.426	13.038	12.678
75°	10	0.043	0.038	0.036	0.034	0.033	0.032	0.031
	20	0.132	0.116	0.109	0.104	0.100	0.097	0.095
	50	0.718	0.628	0.593	0.562	0.541	0.527	0.513
	80	2.710	2.362	2.224	2.106	2.024	1.967	1.916
	90	4.285	3.731	3.516	3.308	3.178	3.088	3.005
	100	6.790	5.900	5.552	5.247	5.036	4.893	4.760

Table 6 Continued

β	GSI	B/H						
		1.0	1.5	2.0	3.0	5.0	10.0	2D
90°	10	0.009	0.007	0.007	0.006	0.006	0.006	0.006
	20	0.024	0.020	0.019	0.017	0.017	0.016	0.015
	50	0.181	0.152	0.141	0.131	0.125	0.120	0.117
	80	0.985	0.831	0.773	0.717	0.689	0.659	0.636
	90	1.729	1.447	1.342	1.254	1.191	1.148	1.110
	100	3.019	2.549	2.340	2.188	2.075	2.003	1.934

3.2 The critical values of ϕ_t and c_t

Fig. 8 shows the effect of B/H on the critical value of the equivalent friction angle ϕ_t for rock slopes under both static and seismic conditions. It can be observed that, the equivalent friction angle ϕ_t stays in a nearly constant value as the ratio of B/H increases. In the 3D failure mechanism (as shown in Fig. 2), the equivalent friction angle ϕ_t is one half of the apex angle for the curvilinear cone and determines the shape of the cone. Whereas, the ratio of B/H has significant influences on the values of variables θ_0, θ_h, r_0'/r_0, and b/H, which determine the location of the curvilinear cone. Therefore, the equivalent friction angle ϕ_t is independent of the ratio of B/H. The ratio of B/H = 3.0 is adopted to further investigate the effects of the parameters m_i and GSI on the values of ϕ_t and c_t.

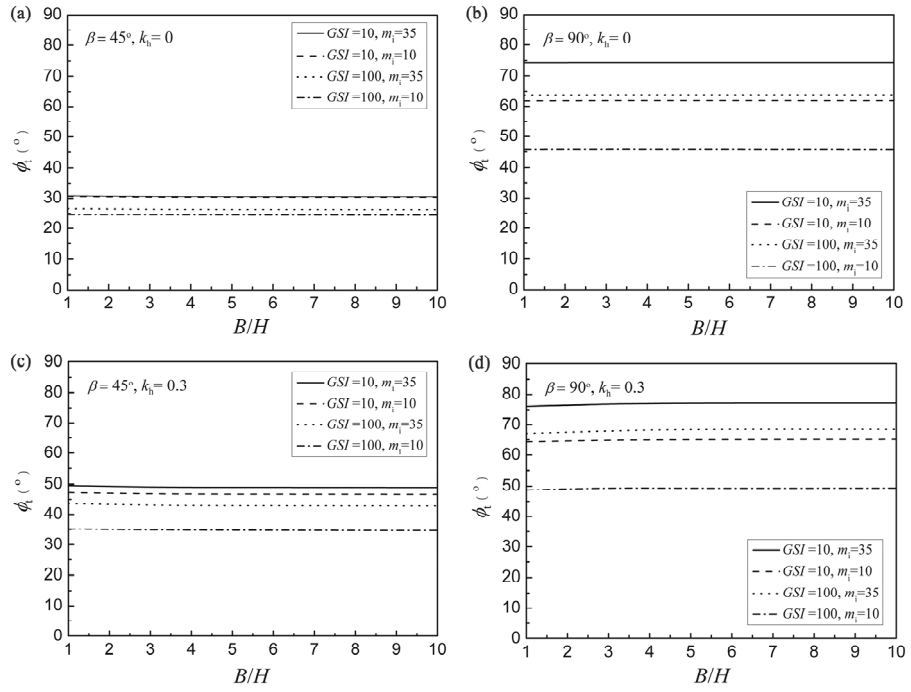

Fig. 8 The effect of B/H on the optimized equivalent friction angle ϕ_t for rock slopes under both static and seismic conditions

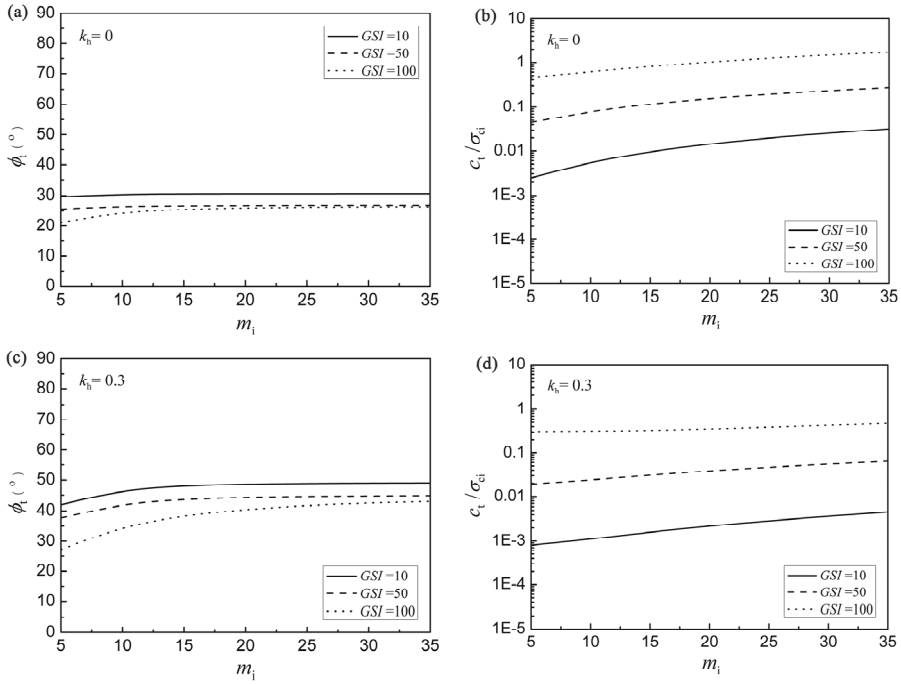

Fig. 9 The effect of m_i on the values of ϕ_t and c_t for gentle rock slopes with $\beta = 45°$

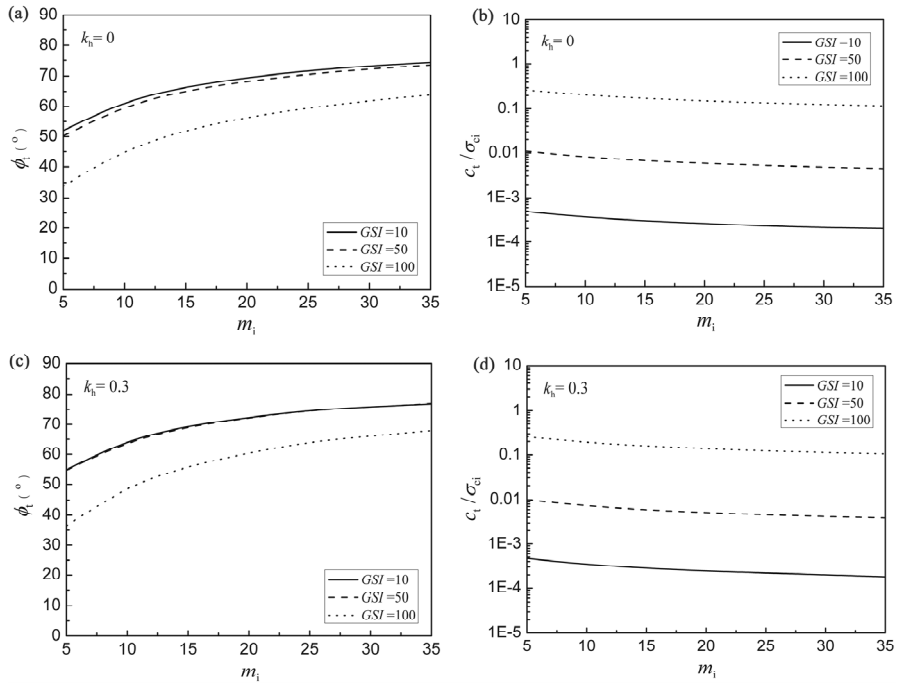

Fig. 10 The effect of m_i on the values of ϕ_t and c_t for steep rock slopes with $\beta = 90°$

Figs. 9 and 10 illustrate the effect of the parameter m_i on the critical values of ϕ_t and c_t for rock slopes with $\beta = 45°$ and 90°, respectively. It can be seen from Fig. 9 that, both the values of ϕ_t and c_t increase with increasing m_i for a gentle slope, which makes the slope more stable as shown in Figs. 3 and 4. For a vertical slope (Fig. 10), the value of ϕ_t increases with increasing m_i, but the corresponding value of c_t decreases. Moreover, it can be found that the value of ϕ_t decreases as *GSI* increases, but the corresponding value of c_t increases.

4. Conclusions

Based on the generalized non-linear HB criterion, this study adopted the tangential technique to develop the upper-bound limit analysis of 3D rock slopes stability under both static and pseudo-static seismic loading conditions. The calculated results presented in the form of graphs and tables demonstrated the influences of 3D geometrical constraint, non-linear strength parameters and seismic acceleration on the stability number and the equivalent strength parameters. These solutions can be used for preliminary assessment on the 3D rock slope stability in design, and provide available data for evaluating other developing methods in the fledgling area of 3D rock slope stability analysis. Regarding the results of this study, the following conclusions can be drawn:

- The stability number of a rock slope decreases with increasing ratio of B/H and the 3D end effect is significant for a rock slope constrained to a narrow width. When the constraint on the width reaches B/H = 10.0, the 3D effect can be neglected in the assessment of the stability of rock slope and the plane-strain analysis is appropriate.
- For 3D rock slopes under static conditions, the stability number increases obviously with the parameter m_i increasing in most cases, but slightly for vertical slopes. When the steep slopes are subjected to seismic excitations, the stability number will tend to decrease as m_i increases, especially for vertical slopes. In this situation, most of the normal stresses along the slip surface are rather small and the shear strength of rock masses will be lower with m_i increasing. Hence, the steep slopes with a bigger m_i will be less stable.
- The ratio of B/H almost has no effect on the critical values of ϕ_t and c_t, but the rock parameters (m_i and *GSI*) and the slope angle (β) have significant effects on them.

Acknowledgments

This study was financially supported by National Key Basic Research Program of China under Grant No. 2015CB057901, the Public Service Sector R&D Project of Ministry of Water Resource of China (Grant No. 201501035-03), the National Natural Science Foundation of China (Grant Nos. 51278382, 51479050, 51508160 and 51378472), the 111 Project (Grant No. B13024), the Fundamental Research Funds for the Central Universities (Grant Nos. 2014B06814, 2014B33414 and B15020060), the Open Foundation of Key Laboratory of Failure Mechanism and Safety Control Techniques of Earth-rock Dam of the Ministry of Water Resources (Grant No. YK913004), and Jiangsu Graduate Scientific Research and Innovation Project (CXZZ13_0242).

References

Carranza-Torres, C. (2004), “Some comments on the application of the Hoek–Brown failure criterion for

intact rock and rock masses to the solution of tunnel and slope problems", *MIR 2004–X Conference on Rock and Engineering Mechanics*, *Torino*, 285-326.
Carranza-Torres, C. and Fairhurst, C. (1999), "The elasto-plastic response of underground excavations in rock masses that satisfy the Hoek–Brown failure criterion", *Int. J. Rock Mech. Min. Sci.*, **36**(6), 777-809.
Chakraborti, S., Konietzky, H. and Walter, K. (2012), "A comparative study of different approaches for factor of safety calculations by shear strength reduction technique for non-linear Hoek–Brown failure criterion", *Geotech. Geol. Eng.*, **30**(4), 925-934.
Chen, W.F. (1975), *Limit Analysis and Soil Plasticity*, Elsevier, Amsterdam, The Netherlands.
Chen, Z.Y. (1992), "Random trials used in determining global minimum factors of safety of slopes", *Can. Geotech. J.*, **29**(2), 225-233.
Chen, W.F. and Liu, X.L. (1990), *Limit Analysis in Soil Mechanics*, Elsevier, Amsterdam, The Netherlands.
Collins, I.F., Gunn, C.I.M., Pender, M.J. and Yan, W. (1988), "Slope stability analyses for materials with a nonlinear failure envelope", *Int. J. Numer. Anal. Methods Geomech.*, **12**(5), 533-550.
Dawson, E., You, K. and Park, Y. (2000), "Strength-reduction stability analysis of rock slopes using the Hoek-Brown failure criterion", *Geotechnical Special Publication*, 65-77.
Fraldi, M. and Guarracino, F. (2009), "Limit analysis of collapse mechanisms in cavities and tunnels according to the Hoek–Brown failure criterion", *Int. J. Rock Mech. Min. Sci.*, **46**(4), 665-673.
Fu, W. and Liao, Y. (2010), "Non-linear shear strength reduction technique in slope stability calculation", *Comput. Geotech.*, **37**(3), 288-298.
Hammah, R.E., Curran, J.H., Yacoub, T.E. and Corkum, B. (2004), "Stability analysis of rock slopes using the finite element method", *Proceedings of the ISRM Regional Symposium*, EUROCK.
Hobbs, D. (1966), "A study of the behaviour of broken rock under triaxial compression and its application to mine roadways", *Int. J. Rock Mech. Min. Sci.*, **3**(1), 11-43.
Hoek, E. (1983), "Strength of jointed rock masses", *Geotechnique*, **33**(3), 187-223.
Hoek, E. (2007), *Rock Mass Properties*, Practical rock engineering, Rocscience Inc. http://www. rocscience.com/hoek/corner/11_Rock_mass_properties.pdf
Hoek, E. and Brown, E.T. (1980), "Empirical strength criterion for rock masses", *J. Geotech. Eng. Div. ASCE*, **106**(GT9), 1013-1035.
Hoek, E., Wood, D. and Shah, S. (1992), "A modified Hoek–Brown failure criterion for jointed rock masses", *Proc. Rock Characterization*, *Symp. Int. Soc. Rock Mech.*: *Eurock*, **92**, 209-214.
Hoek, E., Carranza-Torres, C. and Corkum, B. (2002), "Hoek-Brown failure criterion–2002 edition", *Proceedings of the North American Rock Mechanics Society Meeting*, Toronto, Canada, January, pp. 267-273.
Li, A.J., Merifield, R.S. and Lyamin, A.V. (2008), "Stability charts for rock slopes based on the Hoek-Brown failure criterion", *Int. J. Rock Mech. Min. Sci.*, **45**(5), 689-700.
Li, A.J., Lyamin, A.V. and Merifield, R.S. (2009), "Seismic rock slope stability charts based on limit analysis methods", *Comput. Geotech.*, **36**(1-2), 135-148.
Lin, H., Zhong, W., Xiong, W. and Tang, W. (2014), "Slope stability analysis using limit equilibrium method in nonlinear criterion", *Sci. World J.*
Michalowski, R.L. and Drescher, A. (2009), "Three-dimensional stability of slopes and excavations", *Geotechnique*, **59**(10), 839-850.
Michalowski, R.L. and Martel, T. (2011), "Stability charts for 3D failures of steep slopes subjected to seismic excitation", *J. Geotech. Geoenviron. Eng.*, **137**(2), 183-189.
Michalowski, R.L. and You, L.Z. (2000), "Displacements of reinforced slopes subjected to seismic loads", *J. Geotech. Geoenviron. Eng.*, **126**(8), 685-694.
Saada, Z., Maghous, S. and Garnier, D. (2012), "Stability analysis of rock slopes subjected to seepage forces using the modified Hoek–Brown criterion", *Int. J. Rock Mech. Min. Sci.*, **55**, 45-54.
Sharan, S.K. (2003), "Elastic–brittle–plastic analysis of circular openings in Hoek–Brown media", *Int. J. Rock Mech. Min. Sci.*, **40**(6), 817-824.
Shen, J. and Karakus, M. (2013), "Three-dimensional numerical analysis for rock slope stability using shear strength reduction method", *Can. Geotech. J.*, **51**(2), 164-172.

Shen, J., Karakus, M. and Xu, C. (2013), "Chart-based slope stability assessment using the Generalized Hoek–Brown criterion", *Int. J. Rock Mech. Min. Sci.*, **64**, 210-219.

Sheorey, P.R., Biswas, A.K. and Choubey, V.D. (1989), "An empirical failure criterion for rocks and jointed rock masses", *J. Eng. Geol.*, **26**(2), 141-159.

Yang, X.L. and Qin, C.B. (2014), "Limit analysis of rectangular cavity subjected to seepage forces based on Hoek-Brown failure criterion", *Geomech. Eng.*, **6**(5), 503-515.

Yang, X.L., Li, L. and Yin, J.H. (2004), "Seismic and static stability analysis for rock slopes by a kinematical approach", *Geotechnique*, **54**(8), 543-549.

Yudhbir, Y., Lemanza, W. and Prinzl, F. (1983), "An empirical failure criterion for rock masses", *Proceedings of the 5th ISRM Congress*, *International Society for Rock Mechanics*, Melbourne, Australia, April.

CC